Multipolar effects on the dipolar polarizability of magneto-electric antennas

S. Varault, B. Rolly, G. Boudarham, G. Demésy, B. Stout, and N. Bonod*

CNRS, Aix-Marseille Université, Ecole Centrale Marseille, Institut Fresnel, Campus of Saint Jérôme ,13013 Marseille, France

*nicolas.bonod@fresnel.fr

Abstract: We show the important role played by the multipolar coupling between the illuminating field and magneto-electric scatterers even in the small particle limit ($\lambda/10$). A general multipolar method is presented which, for the case of planar non centrosymmetric particles, generates a simple expression for the polarizability tensor that directly links the dipolar moment to the incident field. The relevancy of this approach is demonstrated by comparing thoroughly the dipolar moments predicted by the method with full numerical calculations.

OCIS codes: (290.5850) Scattering, particles; (160.3918) Metamaterials; (260.3910) Metal optics; (160.4760) Optical properties; (240.6680) Surface plasmons.

References and links

1. C. Enkrich, M. Wegener, S. Linden, S. Burger, L. Zschiedrich, F. Schmidt, J. F. Zhou, T. Koschny, and C. M. Soukoulis, "Magnetic metamaterials at telecommunication and visible frequencies," Phys. Rev. Lett. **95**, 203901 (2005).
2. C. Rockstuhl, F. Lederer, C. Etrich, T. Zentgraf, J. Kuhl, and H. Giessen, "On the reinterpretation of resonances in split-ring-resonators at normal incidence," Opt. Express **14**, 8827–8836 (2006).
3. M. W. Klein, C. Enkrich, M. Wegener, C. M. Soukoulis, and S. Linden, "Single-slit split-ring resonators at optical frequencies: limits of size scaling," Opt. Lett. **31**, 1259–1261 (2006).
4. M. Husnik, M. W. Klein, N. Feth, M. König, J. Niegemann, K. Busch, S. Linden, and M. Wegener, "Absolute extinction cross-section of individual magnetic split-ring resonators," Nat. Photonics **2**, 614–617 (2008).
5. I. Sersic, M. Frimmer, E. Verhagen, and A. F. Koenderink, "Electric and magnetic dipole coupling in near-infrared split-ring metamaterial arrays," Phys. Rev. Lett. **103**, 213902 (2009).
6. N. Guth, B. Gallas, J. Rivory, J. Grand, A. Ourir, G. Guida, R. Abdeddaim, C. Jouvaud, and J. de Rosny, "Optical properties of metamaterials: Influence of electric multipoles, magnetoelectric coupling, and spatial dispersion," Phys. Rev. B **85**, 115138 (2012).
7. G. Boudarham, N. Feth, V. Myroshnychenko, S. Linden, J. García de Abajo, M. Wegener, and M. Kociak, "Spectral imaging of individual split-ring resonators," Phys. Rev. Lett. **105**, 255501 (2010).
8. A. García-Etxarri, R. Gómez-Medina, L. S. Froufe-Pérez, C. López, L. Chantada, F. Scheffold, J. Aizpurua, M. Nieto-Vesperinas, and J. J. Sáenz, "Strong magnetic response of submicron silicon particles in the infrared," Opt. Express **19**, 4815–4826 (2011).
9. A. B. Evlyukhin, C. Reinhardt, and B. N. Chichkov, "Multipole light scattering by nonspherical nanoparticles in the discrete dipole approximation," Phys. Rev. B **84**, 235429 (2011).
10. A. B. Evlyukhin, S. M. Novikov, U. Zywietz, R. L. Eriksen, C. Reinhardt, S. I. Bozhevolnyi, and B. N. Chichkov, "Demonstration of magnetic dipole resonances of dielectric nanospheres in the visible region," Nano Lett. **12**, 3749–3755 (2012).
11. P. Spinelli, M. Verschuuren, and A. Polman, "Broadband omnidirectional antireflection coating based on subwavelength surface mie resonators," Nat. Commun. **3** (2012).
12. B. Rolly, B. Stout, and N. Bonod, "Boosting the directivity of optical antennas with magnetic and electric dipolar resonant particles," Opt. Express **20**, 20376–20386 (2012).

#189044 - $15.00 USD Received 17 Apr 2013; revised 2 Jun 2013; accepted 3 Jun 2013; published 2 Jul 2013

13. J. M. Geffrin, B. García-Cámara, R. Gómez-Medina, P. Albella, L. Froufe-Pérez, C. Eyraud, A. Litman, R. Vaillon, F. González, M. Nieto-Vesperinas, J. Sáenz, and F. Moreno, "Magnetic and electric coherence in forward- and back-scattered electromagnetic waves by a single dielectric subwavelength sphere," Nat. Commun. **3** (2012).
14. S. Person, M. Jain, Z. Lapin, J. J. Saenz, G. Wicks, and L. Novotny, "Demonstration of zero optical backscattering from single nanoparticles," Nano Lett. **13 (4)**, pp 18061809 (2013).
15. Y. H. Fu, A. I. Kuznetsov, A. E. Miroshnichenko, Y. F. Yu, and B. Luk'yanchuk, "Directional visible light scattering by silicon nanoparticles," Nat. Commun. **4** (2013).
16. W. Liu, A. E. Miroshnichenko, D. N. Neshev, and Y. S. Kivshar, "Broadband Unidirectional Scattering by Magneto-Electric Core-Shell Nanoparticles," ACS Nano **6**, 5489–5497 (2012).
17. B. Rolly, B. Bebey, S. Bidault, B. Stout, and N. Bonod, "Promoting magnetic dipolar transition in trivalent lanthanide ions with lossless mie resonances," Phys. Rev. B **85**, 245432 (2012).
18. C. M. Dodson and R. Zia, "Magnetic dipole and electric quadrupole transitions in the trivalent lanthanide series: Calculated emission rates and oscillator strengths," Phys. Rev. B **86**, 125102 (2012).
19. Y. Terekhov, A. Zhuravlev, and G. Belokopytov, "The polarizability matrix of split-ring resonators," Moscow Univ. Phys. Bull. **66**, 254–259 (2011).
20. D. Morits and C. Simovski, "Isotropic negative effective permeability in the visible range produced by clusters of plasmonic triangular nanoprisms," Metamaterials **5**, 162–168 (2011).
21. A. Ishimaru, S.-W. Lee, Y. Kuga, and V. Jandhyala, "Generalized constitutive relations for metamaterials based on the quasi-static lorentz theory," IEEE Trans. Antennas Propag. **51**, 2550–2557 (2003).
22. A. Vallecchi, M. Albani, and F. Capolino, "Collective electric and magnetic plasmonic resonances in spherical nanoclusters," Opt. Express **19**, 2754–2772 (2011).
23. J. Petschulat, C. Menzel, A. Chipouline, C. Rockstuhl, A. Tünnermann, F. Lederer, and T. Pertsch, "Multipole approach to metamaterials," Phys. Rev. A **78**, 043811 (2008).
24. L. Zhou and S. T. Chui, "Magnetic resonances in metallic double split rings: Lower frequency limit and bianisotropy," Appl. Phys. Lett. **90**, 041903 (2007).
25. D. Chigrin, C. Kremers, and S. Zhukovsky, "Plasmonic nanoparticle monomers and dimers: from nanoantennas to chiral metamaterials," Appl. Phys. B **105**, 81–97 (2011).
26. P. de Vries, D. V. van Coevorden, and A. Lagendijk, "Point scatterers for classical waves," Rev. Mod. Phys. **70**, 447–466 (1998).
27. I. Sersic, C. Tuambilangana, T. Kampfrath, and A. F. Koenderink, "Magnetoelectric point scattering theory for metamaterial scatterers," Phys. Rev. B **83**, 245102 (2011).
28. M. Liu, D. A. Powell, I. V. Shadrivov, and Y. S. Kivshar, "Optical activity and coupling in twisted dimer meta-atoms," Appl. Phys. Lett. **100**, 111114 (2012).
29. C. Simovski and S. Tretyakov, "On effective electromagnetic parameters of artificial nanostructured magnetic materials," Photonic. Nanostruct. **8**, 254–263 (2010). Tacona Photonics 2009.
30. F. Capolino, *Theory and Phenomena of Metamaterials* (CRC, 2009).
31. J. Petschulat, J. Yang, C. Menzel, C. Rockstuhl, A. Chipouline, P. Lalanne, A. Tüennermann, F. Lederer, and T. Pertsch, "Understanding the electric and magnetic response of isolated metaatoms by means of a multipolar field decomposition," Opt. Express **18**, 14454–14466 (2010).
32. A. Chipouline, C. Simovskib, S. Tretyakovb, "Basics of averaging of the Maxwell equations for bulk materials," Metamaterials **6**, 77–120 (2012).
33. R. E. Raab and O. L. de Lange, *Multipole Theory in Electromagnetism: Classical, Quantum, and Symmetry Aspects, with Applications* (Oxford University , 2005).
34. I. V. Lindell, A. Sihvola, and S. Tretyakov, *Electromagnetic Waves in Chiral and Bi-Isotropic Media* (Artech House, 1994).
35. P. Mazur, B. Nijboer, "On the statistical mechanics of matter in an electromagnetic field. I," Physica XIX, 971 (1953).
36. P. B. Johnson and R. W. Christy, "Optical constants of the noble metals," Phys. Rev. B **6**, 4370–4379 (1972).
37. C. Rockstuhl, T. Zentgraf, E. Pshenay-Severin, J. Petschulat, A. Chipouline, J. Kuhl, T. Pertsch, H. Giessen, and F. Lederer, "The origin of magnetic polarizability in metamaterials at optical frequencies - an electrodynamic approach," Opt. Express **15**, 8871–8883 (2007).
38. Y. Zeng, C. Dineen, and J. V. Moloney, "Magnetic dipole moments in single and coupled split-ring resonators," Phys. Rev. B **81**, 075116 (2010).
39. G. Demésy, F. Zolla, A. Nicolet, and M. Commandré, "Versatile full-vectorial finite element model for crossed gratings," Opt. Lett. **34**, 2216–2218 (2009).
40. J. D. Jackson, *Classical Electrodynamics*, 3rd ed. (John Wiley & Sons, New York, 1999).
41. P. Grahn, A. Shevchenko, and M. Kaivola, "Electromagnetic multipole theory for optical nanomaterials," New J. Phys. **14**, 093033 (2012).

#189044 - $15.00 USD Received 17 Apr 2013; revised 2 Jun 2013; accepted 3 Jun 2013; published 2 Jul 2013

1. Introduction

Light-matter interactions have traditionally been investigated from the electric field viewpoint on account of the fact that electric dipole transition rates of quantum emitters are typically five orders of magnitude higher than magnetic dipole transitions. Nevertheless, by structuring non magnetic materials at a subwavelength scale, it is possible to create artificial 'atoms' which can resonantly interact with incident light via strong electric and/or magnetic polarizabilities. Split Ring Resonators (SRR) and U-shaped scatterers are certainly the most emblematic photonic components for creating artificial magnetism [1–7]. More recently, dielectric Mie resonators of moderate refractive index ($n \approx 3.5$) have attracted keen interest since they possess both magnetic and electric polarizabilities [8–10] which in turn lead to interesting scattering properties [11–16]. Mie resonators have also been shown to specifically enhance either electric or magnetic local density of states (LDOS) and they could serve as efficient optical antennas for increasing the magnetic transition rates of trivalent lanthanide ions [17, 18]. These recent advances concerning the scattering and LDOS properties of dielectric Mie resonators were facilitated by an accurate knowledge of their complex dipolar and multipolar response functions. It should prove interesting to extend these findings to the case of metallic magneto-electric scatterers. However, although the calculation of induced polarization moments is well known for spherical particles, it can prove tricky for the case of highly asymmetric particles. The computation of a polarizability tensor for arbitrarily shaped particles is therefore a crucial step in the design and understanding of both metamaterials and optical antennas.

The method of counter-propagating waves [19–22] is often proposed to numerically compute the polarizability tensor $\bar{\bar{\alpha}}$ of scatterers. This method aims at determining the various components of the polarizability tensor by illuminating the object with a superposition of plane waves, in such a way that the resulting excitations take the form of purely electric or magnetic fields polarized along one of three orthogonal directions (the principal axes of the scatterer), thereby permitting the determination of the corresponding column of the polarizability tensor.

Other approaches have also been adopted which rely on numerical descriptions of the scatterer in the dipole approximation [23–25]. The point scattering technique [26] assumes that the constitutive polarizabilities are described by a Lorentzian spectral response which linearly links the induced dipoles to the excitation field, and adjusts the corresponding parameters to fit experimental measurements for a given incidence [27]. Lagrange and hybridization models are also used to describe optical activity in nanoparticle dimers with quite good results for simple shapes like nanorods [25, 28], whose can be well described with a single oriented electric dipole moment.

The above methods are applicable for symmetric particles for which the dependence on propagation direction can be disregarded. Nevertheless, their straightforward application to strongly asymmetric particles or nanoclusters may show some limitations if the coupling of the scatterer with the incident field is not manipulated with a sufficient care. In particular, it has been shown that multipolar contributions of the incident field can influence the polarizability tensor of coupled particles or asymmetric meta-atoms [29, 30], even in situations where the overall scattering response remains essentially dipolar [31]. Recently, a description in terms of microscopic effects was provided to explain the multipolar contribution of the coupling between an incident field and a meta-atom [32]. Hence, it is important to consider such coupling aspects, in addition to previous scattered field analysis based on multipolar decompositions upon spherical wave basis [31].

We study in this paper how such multipolar effects contribute to the creation of induced electric and magnetic dipoles for non-centrosymmetric planar scatterers illuminated from far-field region, and we derive a correction to the classical dipolar polarizability tensor that takes into account such contributions. We show that their full profile can only be explained by taking

#189044 - $15.00 USD Received 17 Apr 2013; revised 2 Jun 2013; accepted 3 Jun 2013; published 2 Jul 2013

into account spatial derivatives of the excitation field according to the multipolar theory [33]. As a typical example, we calculate the dipolar moments of a single U-shaped resonator and propose a method to determine an effective dipolar polarizability tensor that takes into account the multipolar contributions of the illuminating field in the case of a far field illumination. We calculate for arbitrary incidences the polarizability tensor derived with our method. We finally compare the results with full vector finite element numerical calculations to demonstrate the accuracy of this method.

2. Principle

The polarizability tensor $\overline{\overline{\alpha}}$ of a dipolar particle illuminated by an electromagnetic field ($\mathbf{E}^0$,$\mathbf{H}^0$) is generally cast [34]:

$$\begin{bmatrix} \mathbf{p} \\ \mathbf{m} \end{bmatrix} = \underbrace{\begin{bmatrix} \overline{\overline{\alpha}}^{ee} & \overline{\overline{\alpha}}^{em} \\ \overline{\overline{\alpha}}^{me} & \overline{\overline{\alpha}}^{mm} \end{bmatrix}}_{\overline{\overline{\alpha}}} \begin{bmatrix} \mathbf{E}^0 \\ \mathbf{H}^0 \end{bmatrix} \tag{1}$$

where $\overline{\overline{\alpha}}^{ee}$ and $\overline{\overline{\alpha}}^{mm}$ describe direct electric and magnetic effects while $\overline{\overline{\alpha}}^{em}$ and $\overline{\overline{\alpha}}^{me}$ refer to the electromagnetic and magneto-electric polarizability tensors and render the possible bi-anisotropic character of the scatterer. Equation (1) predicts a linear dependence on the local incident field components, a property which is true when moments of a given angular momentum order are only induced by excitation fields of the same order. This situation is usually satisfied for highly symmetric particles, but proves questionable in full multipolar theory for particles of arbitrary form, wherein spatial derivatives of the excitation field can also contribute to the dipolar responses through [33, 35]:

$$\begin{aligned} p_i &= \alpha_{ij}^{ee} E_j^0 + a_{ijk} \nabla_k E_j^0 + \alpha_{ij}^{em} H_j^0 + b_{ijk} \nabla_k H_j^0 + \cdots \\ m_i &= \alpha_{ij}^{me} E_j^0 + c_{ijk} \nabla_k E_j^0 + \alpha_{ij}^{mm} H_j^0 + d_{ijk} \nabla_k H_j^0 + \cdots \end{aligned} \tag{2}$$

where each subscript i, j, and k corresponds to one space coordinate x, y , or z, and where the dipolar (resp. quadrupolar) coupling terms are given by the tensors $\overline{\overline{\alpha}}^{ee}$, $\overline{\overline{\alpha}}^{mm}$, $\overline{\overline{\alpha}}^{em}$, and $\overline{\overline{\alpha}}^{me}$ (resp. $\overline{\overline{a}}$, $\overline{\overline{b}}$,$\overline{\overline{c}}$, and $\overline{\overline{d}}$). Equation (2) introduces a dependence on the wavevector orientation appearing along any non-symmetric direction of the particle or nano-cluster.

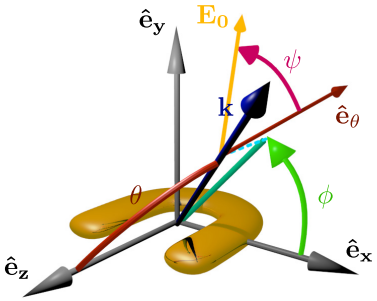

Fig. 1. Schematic of the studied U-shaped ring resonator and definition of the referential cartesian coordinate system. The U-shaped resonator is made of gold [36] and embedded in air. The resonator has equal lateral dimensions l_x and l_z of 200nm and a thickness l_y of 25nm, while the gap width is set to 60nm.

#189044 - $15.00 USD Received 17 Apr 2013; revised 2 Jun 2013; accepted 3 Jun 2013; published 2 Jul 2013

In the following, we aim to illustrate how multipolar couplings affect the induced dipolar moments for U-shaped resonators described in Fig. 1, even for particle sizes as small as $\lambda/10$. We proceed by a systematic inspection of the induced dipolar electric and magnetic moments for different incidence directions and polarizations. We perform the computations in a cartesian coordinate system that matches the principal axes of the resonator to obtain simplified (presumably diagonal) expressions of the direct electric and magnetic tensors $\overline{\overline{\alpha}}_{ee}$ and $\overline{\overline{\alpha}}_{mm}$ in Eq. (1) and we place the origin at the center of mass of the resonator [37,38]. The field scattered by the object illuminated by a plane wave can be computed using an appropriate formulation of the Finite Element Method (FEM). This 3D vector formulation relies on the use of second order edge elements and perfectly matched layers [39]. The current density $\mathbf{J}_{vol}(\mathbf{r})$ is readily deduced from the total field inside the scatterer. The induced electric and magnetic dipole moments are finally computed according to the following standard definitions [40]:

$$\begin{aligned} \mathbf{p} &= +\tfrac{1}{j\omega}\int_{V_s}\mathbf{J}_{vol}(\mathbf{r})\,dv \\ \mathbf{m} &= -\tfrac{1}{2}\int_{V_s}\mathbf{r}\times\mathbf{J}_{vol}(\mathbf{r})\,dv \end{aligned} \tag{3}$$

where the integration is performed over the entire volume V_s of the scatterer. The induced dipolar moments could also be computed through a multipolar decomposition [41] of the field radiated by the scatterer. This method can yield more accurate results for scatterers that poorly verify the quasi-static approximation. However, a comparison between the two approaches shows that Eq. (3) provides accurate results for the scatterer under study.

We next proceed with a systematic study of the optical response of the U-shaped resonator to illustrate the effect of multipolar contributions to the dipolar response of the scatterer. We will show that the quadrupole tensors in Eq. (2) simply reduce to scalars that in the end, and in the particular case of the U-shaped resonator, lead to a corrected expression of the polarizability tensor which depends on the angle of incidence θ. This new formulation of the polarizability tensor will then be applied to Eq. (1) to obtain the induced dipolar moments for a given incidence direction. It will finally be shown that this formulation, obtained under specific illumination conditions, is able to accurately predict the dipolar moment for arbitrary directions of incidence.

3. Expression of the corrected polarizability tensor

For the scatterer of Fig. 1, we first plot the extinction cross-section in the case of normal incidence in Fig. 2. In the spectral domain considered here, we found the first three resonances to occur at λ_1=1375nm, λ_2=790nm, and λ_3=630nm. The first and third resonances correspond to odd modes (magnetic modes) and are excited by electric fields parallel to the gap (blue curve in Fig. 2), while the second resonance, associated with an even mode (electric mode), is excited with a polarization perpendicular to the gap (black curve in Fig. 2) [37]. From here on, we focus on the resonance λ_1, at which the magnetic behavior of U-shaped resonators first appears and for which scatterer response remains predominantly dipolar [31].

To illustrate our approach to deduce the contributing polarizabilities in Eq. (2), we study the induced electric dipole moments for two different incidence conditions. The electric field is defined using the polar and azimuthal angles θ and ϕ together with a polarization angle, ψ, defined in Fig. 1. The electric field can be cast:

$$\mathbf{E_0}(\mathbf{r}) = \begin{cases} +\cos\psi\cos\theta\cos\phi - \sin\psi\sin\phi \\ +\cos\psi\cos\theta\sin\phi + \sin\psi\cos\phi \\ -\cos\psi\sin\theta \end{cases} \tag{4}$$

#189044 - $15.00 USD Received 17 Apr 2013; revised 2 Jun 2013; accepted 3 Jun 2013; published 2 Jul 2013

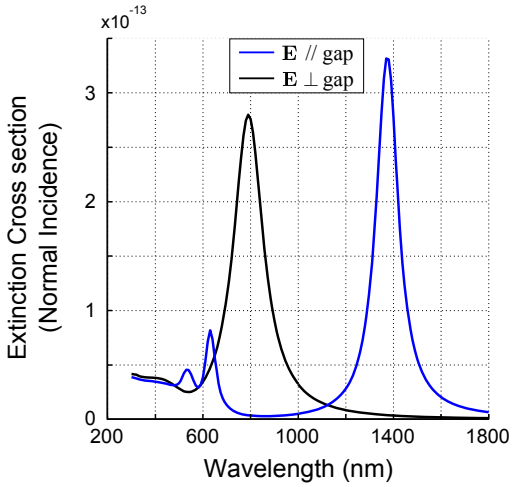

Fig. 2. Extinction cross-section for a single U-shaped resonator at normal incidence for an electric field parallel (black) and normal (blue) to the gap, i.e along and perpendicular to $\hat{\mathbf{e}}_\mathbf{x}$ according to the notations in Fig. 1.

and the magnetic field is simply obtained by $\mathbf{H_0} = \mathbf{k} \times \mathbf{E_0}$, where $\mathbf{k}$ is the incident wave vector. According to the highly subwavelength thickness of the resonator, we neglect all effects of the field gradients along this direction, implying $t_{ijy} \approx 0$, with t=(a,b,c,d). Furthermore, and as a consequence of the high symmetry (resp. asymmetry) of the structure along the yOz (resp. xOy) plane, we assume $t_{ijx} \ll t_{ijz}$ for plane wave incidences with a phase reference matching a symmetry axis of the structure.

We first consider the case of a plane wave incidence whose wavevector lies in the yOz plane, and we rotate the incidence direction around the x axis. The incident electric field is polarized along the x axis (parallel to the gap) which consists in letting θ vary while setting (ϕ,ψ)=(+π/2,-π/2). According to Eqs. (2) and (4), and up to the magnetic quadrupole order, the induced electric dipole moment is:

$$\begin{aligned} p_x^{yOz} &= \alpha_{xx}^{ee} + a_{xxz}^{yOz} \cos\theta \\ &+ \alpha_{xy}^{em} \cos\theta \\ &+ b_{xyz}^{yOz} \cos^2\theta + b_{xzz}^{yOz} \sin\theta \cos\theta \end{aligned} \tag{5}$$

while the other components p_y and p_z remain negligible (we carefully verified this result numerically).

After numerically computing the induced electric moment as a function of θ using Eq. (3), we can use a least square fitting algorithm to quantify the respective contributions of the different polarizabilities. It turns out that no dependence in $\sin\theta\cos\theta$ exists for this illumination condition, and we consequently set $b_{xzz}^{yOz} \approx 0$. This configuration alone remains however insufficient to separately deduce α_{xy}^{em} and a_{xxz}^{yOz} since they are both related to the same cosine function, and we need another illuminating condition to quantify their respective contributions. We next consider an incidence lying in the xOz plane, and we set the magnetic field direction normal to the resonator plane. We now rotate the incidence direction around the y axis by varying θ while

#189044 - $15.00 USD Received 17 Apr 2013; revised 2 Jun 2013; accepted 3 Jun 2013; published 2 Jul 2013

setting (ϕ,ψ)=(0,0). The induced electric dipole moment hence reduces to:

$$\begin{aligned} p_x^{xOz} &= \alpha_{xx}^{ee}\cos\theta \\ &+ a_{xxz}^{xOz}\cos^2\theta + a_{xzz}^{xOz}\sin\theta\cos\theta \\ &+ \alpha_{xy}^{em} + b_{xyz}^{xOz} \end{aligned} \tag{6}$$

and a fitting procedure similar to the previous case gives $a_{xzz}^{xOz} \approx 0$. Only four polarizabilities are then relevant for both Eqs. (5) and (6), namely α_{xx}^{ee}, α_{xy}^{em}, a_{xxz}^{yOz}, and b_{xyz}^{xOz}.

Using simple linear combinations of Eqs. (5) and (6) together, we can finally discriminate the relative contributions of different polarizabilities related to the same function, i.e α_{xy}^{em} and a_{xxz}^{yOz} in Eq. (5), or α_{xy}^{em} and b_{xyz}^{xOz} in Eq. (6). For example, summing up or subtracting the electric dipole moment induced for a forward propagating wave $p_x(\theta)$ and its backward propagating counterpart $p_x(\theta+\pi)$ while keeping a constant polarization will give for the two incidence planes previously discussed:

$$yOz \Rightarrow \begin{cases} p_x(\theta)+p_x(\theta+\pi) &= 2\left(\alpha_{xx}^{ee} + b_{xyz}^{yOz}\cos^2\theta\right) \\ p_x(\theta)-p_x(\theta+\pi) &= 2\left(\alpha_{xy}^{em} + a_{xxz}^{yOz}\right)\cos\theta \end{cases} \tag{7}$$

$$xOz \Rightarrow \begin{cases} p_x(\theta)+p_x(\theta+\pi) &= 2\left(\alpha_{xy}^{ee} + a_{xxz}^{xOz}\cos^2\theta\right) \\ p_x(\theta)-p_x(\theta+\pi) &= 2\left(\alpha_{xx}^{ee} + b_{xyz}^{xOz}\right)\cos\theta \end{cases} \tag{8}$$

From the numerical computation of the induced electric dipolar moment for the aforementioned incidence conditions and using a least square fitting procedure, we can now easily deduce α_{xx}^{ee} and b_{xyz} from the first equation in Eq. (7), while Eq. (8) will give α_{xy}^{em} and a_{xxz}. Numerical results further show that the coefficients deduced from the first equation of Eqs. (7) also verifies the second equation of Eqs. (8), and vice versa, ensuring that the relations $a_{xxz}^{yOz} = a_{xxz}^{xOz}$ and $b_{xyz}^{yOz} = b_{xyz}^{xOz}$ are satisfied.

A similar approach regarding the magnetic dipole moments for incidence planes *xOz* and *yOz* allows the calculation of the parameters α_{yx}^{me}, α_{yy}^{mm}, c_{yxz}, and d_{yyz} that appear in Eq. (9). Since we investigate here only the first resonance, we consider that the electric polarizability α_{zz} parallel to the arms of the U-shape is constant, as this element describes the effect of the second mode of the resonator which is not resonant at this frequency.

The assumptions introduced at the beginning of this section concerning the symmetry of the resonator and the incidence type, together with the previous numerical analysis, lead to the conclusion that the relevant polarizabilities in the tensors relative to second order effects in Eqs. (2) all reduce to scalars. Consequently, we can associate the multipolar contribution on the dipolar moment of the scatterer as corrective terms to the usual dipolar polarizabilities as defined by Eq. (1). Hence, all dipolar effects for this first resonance λ_1 can be described by a polarizability tensor of the form:

$$\bar{\bar{\alpha}}_{cor} = \begin{bmatrix} \alpha_{xx}^{ee} + a_{xxz}\cos\theta & 0 & 0 & 0 & \alpha_{xy}^{em} + b_{xyz}\cos\theta & 0 \\ 0 & 0 & 0 & 0 & 0 & 0 \\ 0 & 0 & \alpha_{zz}^{ee} & 0 & 0 & 0 \\ 0 & 0 & 0 & 0 & 0 & 0 \\ \alpha_{yx}^{me} + c_{yxz}\cos\theta & 0 & 0 & 0 & \alpha_{yy}^{mm} + d_{yyz}\cos\theta & 0 \\ 0 & 0 & 0 & 0 & 0 & 0 \end{bmatrix} \tag{9}$$

#189044 - $15.00 USD Received 17 Apr 2013; revised 2 Jun 2013; accepted 3 Jun 2013; published 2 Jul 2013

We must now quantitatively determinate all the parameters included in this corrected polarizability tensor.

4. Numerical determination of the polarizability tensor

We present in Fig. 3 the dipolar moments numerically computed via Eq. (3) for the two incidence cases described previously. The electric dipole moment perpendicular (resp. parallel) to the gap $p_x(\theta)$ (resp. $p_z(\theta)$) is plotted in red (resp. blue), while the magnetic dipole moment is plotted in green. The full and dotted curves denote the real and imaginary parts of those quantities obtained from FEM computations. For comparison, we plot with black markers in the same graph the results deduced from Eqs. (7) and (8) for $p_x(\theta)$ (and similar equations for $p_z(\theta)$ and $m_y(\theta)$ which are not detailed here for clarity concerns).

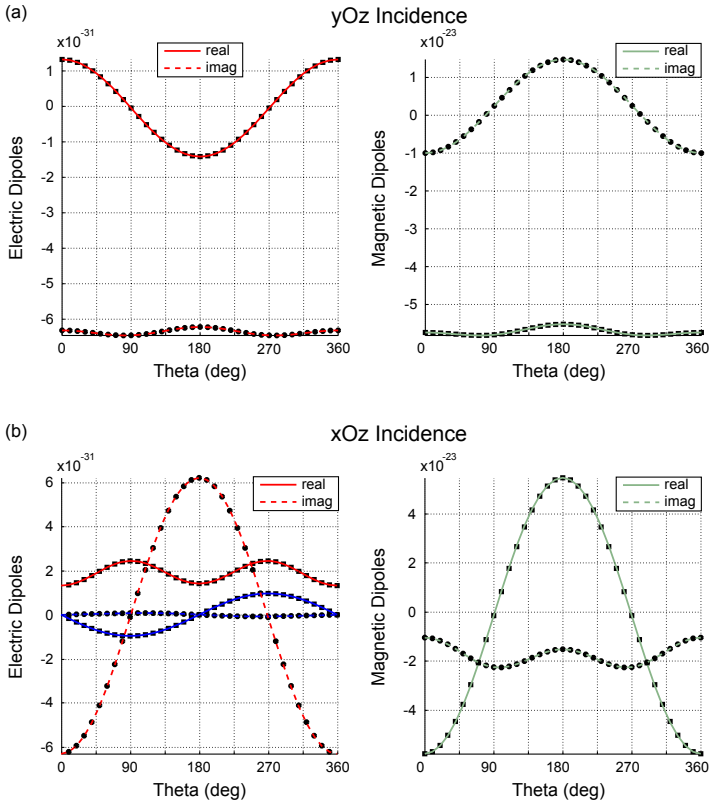

Fig. 3. Real (solid line) and imaginary (dashed line) parts of the induced dipolar moments $p_x(\theta)$ (red), $p_z(\theta)$ (blue) and $m_z(\theta)$ (green) calculated with Eq.3 for the two conditions of incidence used to determine the polarizabilities in Eq. (2). The dipolar moments obtained through the retrieval procedure are indicated with black markers. Planes of incidence *yOz* (a) and *xOz* (b).

We observe in Fig. 3 that the dipolar moments obtained by calculating Eq. (3) with FEM follow a square cosine profile that cannot be predicted by considering the formulation of Eq. (1) which only involves scalar dipolar polarizabilities. This result highlights the quantitative influence of the spatial derivative of the fields on the dipolar moments through the square cosine

#189044 - $15.00 USD Received 17 Apr 2013; revised 2 Jun 2013; accepted 3 Jun 2013; published 2 Jul 2013

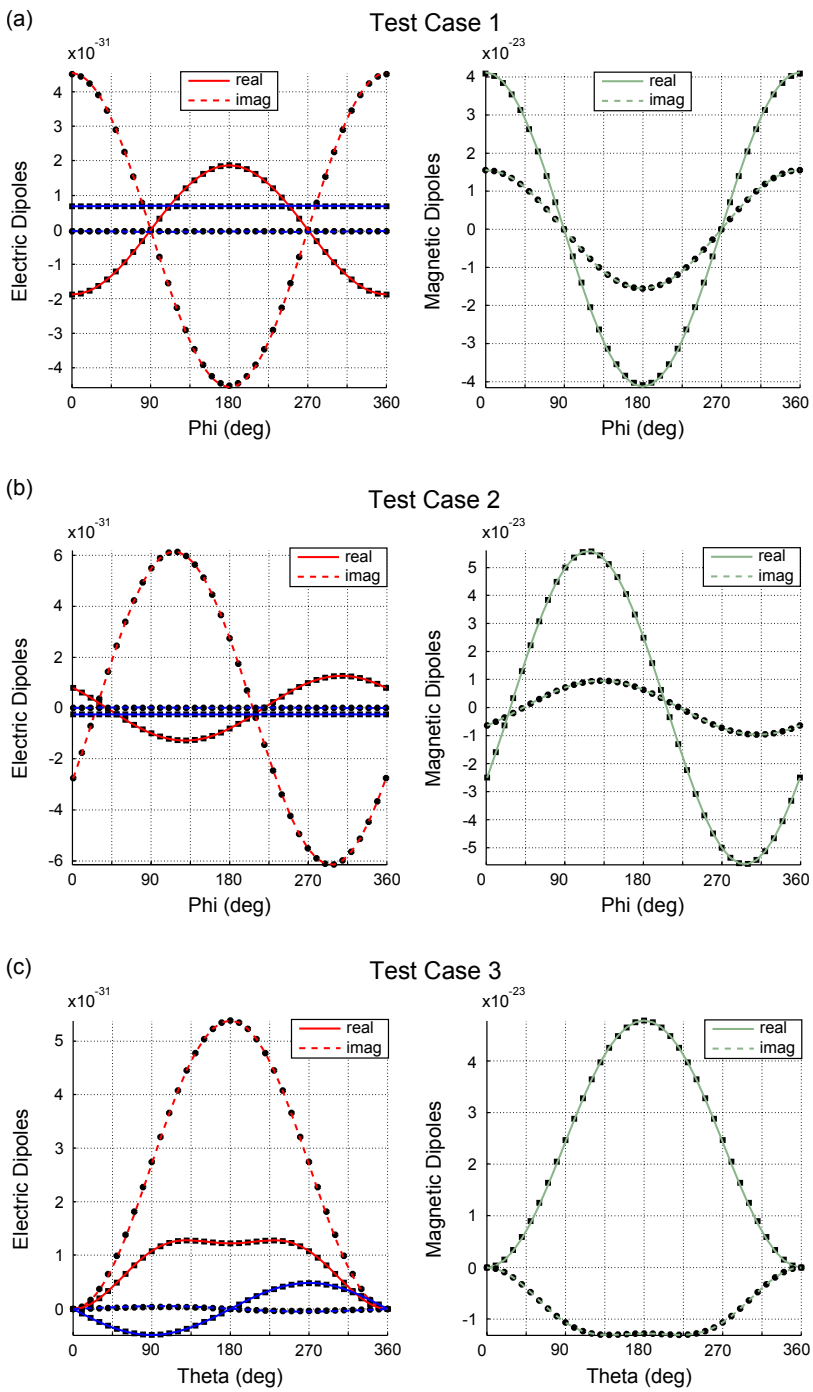

Fig. 4. Real (solid line) and imaginary (dashed line) parts of the induced dipolar moments as a function of incidence. (a) Test case 1 ($\theta = \pi/4$, $\psi = \pi$). (b) Test case 2 ($\theta = \pi/6$, $\psi = \pi/3$). (c) Test case 3 ($\phi = \pi/6$, $\psi = \pi/3$).

#189044 - $15.00 USD Received 17 Apr 2013; revised 2 Jun 2013; accepted 3 Jun 2013; published 2 Jul 2013

functions appearing in Eqs. (7), (8). We can also observe that for a wave propagating along the *z* axis, the induced moments depend on the propagation direction, *i.e.* the dipolar moment obtained at $\theta = 0^\circ$ or 180° are different. Actually, for such a case, the gap is standing either at the back or the front of the scatterer (with respect to the propagation direction) leading to different microscopic charge distributions and near field distributions. These deviations observed in the induced moments as a modification of the coupling mechanism with the excitation field even for particles as small as $\lambda/10$ are fully taken into account by the spatial derivatives in Eqs. (2). One can note that for a wave propagating normal to the resonator plane (*y* axis), or parallel to the gap (*x* axis), no difference can be observed between the two counter propagating directions, that is a consequence of the high symmetry property of the scatterer under these illuminations. More precisely, it can be observed that m_z and p_z are respectively symmetric and anti-symmetric with respect to the $\theta = 180^\circ$ axis. This difference results from the fact that the incident magnetic field component H_z is not modified when modifying θ in the *xOz* incidence plane, while the sign of the electric field component E_z is. Those results tend to valid the assumptions made according to the most relevant spatial derivatives of the excitation field involved in the dipolar response of the particle.

However, to verify the general nature of the corrected dipolar polarizability tensor in Eq. (9) that we obtained under specific illumination conditions, we need to verify its accuracy in arbitrary incidence conditions. For that purpose, we numerically compute the induced dipolar moments using Eq. (3) for oblique incidence that we compare to the induced dipolar moments directly predicted from Eq. (1) when substituting the usual polarizability tensor $\overline{\overline{\alpha}}$ by the corrected tensor $\overline{\overline{\alpha}}_{cor}$ given in Eq. (9) (Fig. 4(a)-4(c)). As in Fig. 3, the colored curves represent the FEM results while black markers represent the semi-analytical derivations.
We observe a linear relation between the induced moments and the excitation field as ϕ is varied (Fig. 4(a)-4(b)). Let us remind that angle ϕ refers to the out-of-plane rotation around the scatterer, and according to our previous assumptions regarding the symmetry of the resonator together with incidence conditions, this linearity was expected. However, for rotations about the in-plane angle θ, which bears the asymmetry information of the scatterer, such linearity does not hold and we can notice in Fig. 4(c) drastic changes in the behavior of the induced moments as a function of θ.

This plot evidences the accuracy and the relevancy of the method derived in this study since both approaches fit very precisely at all incidence angles. It means that the corrected polarizability tensor based on the multipole theory formulation provides a general description of the dipolar response of planar SRR-based resonators illuminated from far field area. This method allows for the derivation of a polarizability tensor that does not depend on the angle of incidence, as required for local models [29], in the sense that all the parameters numerically determined in this section only depend on the incident wavelength. The non-trivial angular variations of the induced moments observed in the FEM results are explained and accurately reproduced when considering the multipolar coupling effects that are described by higher order polarizability tensors related to the spatial derivatives of the excitation field. However, in the specific case of U-shaped resonators, those higher order polarizabilities reduce to scalars resulting in a simplified expression of the polarizability tensor in which each scalar polarizability is angle-dependant, according to Eq. (9). It must be pointed out that multipolar contributions are more important around resonances of the scatterer and a similar behavior occurs for smaller structures since the resonance wavelength scales according to the in-plane size dimensions.

#189044 - $15.00 USD Received 17 Apr 2013; revised 2 Jun 2013; accepted 3 Jun 2013; published 2 Jul 2013

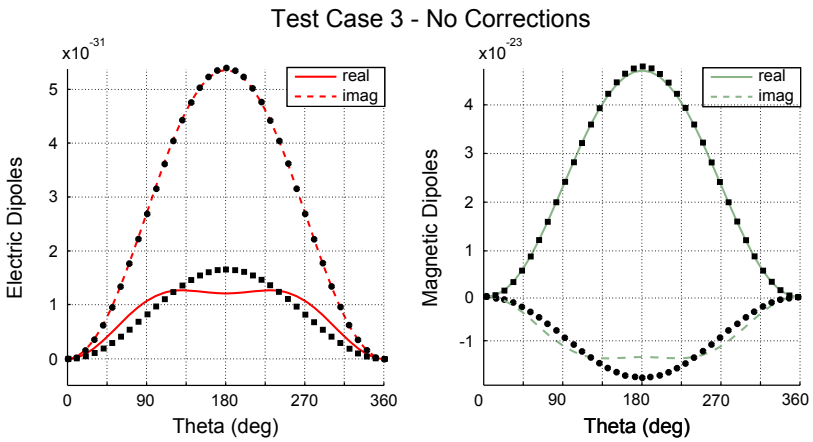

Fig. 5. Real (solid line) and imaginary (dashed line) parts of the induced dipolar moments as a function of incidence in the configuration of Fig. 4(c) by using the non-corrected polarizability tensor of Eq. (1)

In order to quantify the influence of the multipolar effects on the dipolar moments, we finally compute the dipolar polarizabilities alone by considering a tensorial formulation analog to Eq. (1) and assuming a linear dependence between the induced moments and the excitation field. The results displayed in Fig. 5 confirm the mismatch with the FEM results when the higher order corrective parameters that describe the asymmetry of the resonator are neglected.

5. Conclusion

We systematically studied the induced dipolar moments for a U-shaped resonator under far-field illumination and proposed a multipolar based correction to the classically employed dipolar polarizability tensor. We do not operate a multipolar decomposition on the field scattered by the structure, but we analyze how the multipolar coupling between the incident field and the resonator affects the dipolar response of non-centrosymmetric nanoparticles. The importance of the asymmetry on the multipolar coupling is confirmed in the case of a U-shaped planar resonator by the fact that the corresponding corrective terms only play a role when the in-plane rotation angle (which bears the asymmetry) is varied. The relevant quadrupolar tensors are linked to the direct quadrupole-quadrupole coupling, whose influence is found to be very small in the radiated field. Nevertheless, they still impact the scattering process thanks to the perturbation they provoke on the dipolar response: a purely dipolar-dipolar response would present identical induced moments for a backward or forward propagating wave relative to the gap position, contrary to what is observed in this study. We limited this study to the case of a far field incidence which allowed us to reveal multipolar effects on the dipolar response of the scatterer in a simple way. Nevertheless, we believe that this analysis opens the way to the case of near-field illuminations and calculation of local density of states of magneto-electric scatterers.

Acknowledgments

The authors acknowledge Redha Abdeddaim, Victor Grigoriev and Bruno Gallas for stimulating discussions. This research was funded by the French Agence Nationale de la Recherche under Contract No. ANR-11-BS10-002-02 TWINS.

#189044 - $15.00 USD Received 17 Apr 2013; revised 2 Jun 2013; accepted 3 Jun 2013; published 2 Jul 2013